



24th COBEM - 2017



24th ABCM International Congress of Mechanical Engineering
December 3-8, 2017, Curitiba, PR, Brazil

COBEM-2017-2217

COMPUTACIONAL ANALYSIS USING CFD ON PERFORMANCE OF A CENTRIFUGAL PUMP IMPELLER

Ana Rafaelly Amaral Bezerra

Sandi Itamar Schafer de Souza

Universidade Federal do Rio Grande do Norte, Natal, Brazil
rafaellyamarall@hotmail.com
sandi@ufrnet.br

Amanda Braun Barbosa Araújo

Braun.amanda.barbosa@gmail.com

Abstract. Centrifugal pumps are widely used in many industrial applications and they are usually considered the main component of the system, as is the case of pumps for petroleum production through the Electrical Submersible Pump. The comprehension of the components behavior is indispensable for the development, and improvement of be more efficient, reliable and economical systems. However, the analysis of the internal flow of a centrifugal pump is highly complex. This analysis and the determination of the operational conditions can be supported by numerical simulation, using Computational Fluid Dynamics (CFD) techniques, which allows the prediction of flow behavior with off-design conditions, providing reduction of costs and time. This paper presents numerical simulations performed in the computational model of a pump impeller in order to obtain the preliminary results of the numerical models applied by the ANSYS CFX code. With the results, it was possible to obtain the impeller head characteristic curve and compare it with the analytical curve obtained, also making an evaluation of the flow through the study of meridional profiles for the selection of the pressure conditions and the velocity inside of the impeller.

Keywords: Centrifugal Pumps, Computational Fluid Dynamics, Numerical Simulation.

1. INTRODUCTION

The centrifugal pumps are devices that provide kinetic-energy to the fluid converting into pressure energy. This transformation occurs by the rotating axis coupled to a disk with blades that receives the fluid through its center and pushes to the periphery by the action of centrifugal force (Mattos and Falco, 1998). The main components of this device are the impeller and the casing, which the last one can be a volute or a diffuser with blades.

In the industry in general, the centrifugal pumps are important, especially when applied to process which evolves high flow pumping. In this manner, it is essentially the study and the analysis in details, starting from the design stage to the performance of the device, in order to improve the pumps systems and making them increasingly efficient and economical.

In recent years, the use of Computational Fluid Dynamics (CFD) in centrifugal pump simulations has been increasing considerably because of its high accuracy compared with experimental data. These techniques have great potential for application and are widely used in centrifugal pump simulations that become a fundamental step in the design of this device. The CDF simulation allows predicting the flows behavior in hydraulic machines and consequently their operational characteristics with off-design conditions, providing reduction of costs and time of development of the project.

The objective of this work is to simulate by numerical method the single phase flow inside the impeller, using ANSYS CFX code, this leads to the results of head characteristic curve and fluid flow pattern.

2. THEORETICAL REFERENCE

The theoretical study of the flow of liquids through the impeller is done by velocity vectors, which places the velocity triangles. According to Segala (2010), analyzing the velocity triangles and considering the shaft torque as a function of the components of the flow velocity at the input and output of the impeller, the energy transfer rate, how the

flow enters and leaves the impeller through the shape of the blades and the flow rate, that can be obtained by the magnitude of the energy transferred to the impeller in units of length, so the head is shown in Eq. (1).

$$H = \frac{U_2}{g} \left(U_2 - \frac{\dot{Q}}{A_2} \cot g(\beta_2) \right) \quad (1)$$

where g is the gravitational constant, U_2 is the tangential velocity in the impeller output section, β_2 is outlet angle impeller, \dot{Q} is the flow rate and A_2 is the outlet area of the impeller.

Equation (1) shows the main operational characteristics of the pump, such as flow, geometry and rotation. Thus, it is possible to affirm that the head varies linearly with the increase of the flow rate.

Actually, the use of CFD techniques has been increasingly disseminated through its application in works which involves the most diverse areas. It occurs because of the techniques employed have as advantages time and costs saving of experiments and tests, allowing the domain chosen for analysis to be studied in real dimensions, whereas in experiments, prototypes on the reduced scales are often utilized. In addition, the results obtained through the simulations present great versatility and reliability.

Computational Fluid Dynamics (CFD) consists of analyzing and solving systems of differential equations that govern the fluid flow to obtain numerical solutions through computational simulations (Maitelli, 2010).

The equation system mentioned are the continuity equation and the Navier-Stokes equations, according to Wenzel (2010), when starting from governing equations, substituting them for the sum of their means and fluctuations also doing the operation of the average of the equations, defined by the Eq. (2) and Eq. (3).

$$\overline{\frac{\partial u_i}{\partial x_i}} = 0 \quad (2)$$

$$\overline{\frac{\partial u_i}{\partial t}} + \overline{u_j \frac{\partial u_i}{\partial x_j}} = -\frac{1}{\rho} \frac{\partial \overline{p}}{\partial x_i} + \frac{\partial}{\partial x_j} \left(\nu \left(\frac{\partial \overline{u_i}}{\partial x_j} \right) - \overline{u_i u_j} \right) + \overline{f_i} \quad (3)$$

where t is the time, x is the length, ν is the viscosity, $\overline{u_i}$ is the velocity, \overline{p} is the pressure, $\overline{f_i}$ is the body force and $\overline{u_i u_j}$ is the Reynolds stress tensor with the i and j subscripts label represents the coordinate system.

3. METHODOLOGY

In the methodology is presented the impeller geometry model of a centrifugal pump as well as the generation of the mesh and the contour conditions applied, which are required for the accomplishment of the simulations.

3.1 Geometry model

Performing simulations using CFD is indispensable to obtain a geometric model that is compatible with the real physical phenomenon to be simulated. Simulations were performed for a partially open impeller whose the design was sent by Laboratório de Máquinas de Fluxo of URI/RS. The geometry was obtained from an available pump reducing the impeller diameter to provide a higher efficiency possible to the established conditions for the pump. Table 1 shows the dimensions and properties for the available impeller and the new geometry obtained. The three-dimensional model is shown in Fig. 1.

Table 1. Dimensions and properties from the old and the new geometry.

Old geometry	n(rpm)	D ₂ (mm)	D ₁ (mm)	b ₂ (mm)	b ₁ (mm)	β ₂ °	β ₁ °	P(c.v)
	3495	127,5	24,5	5,5	5,5	11,6	46,5	1
New geometry	n(rpm)	D ₂ (mm)	D ₁ (mm)	b ₂ (mm)	b ₁ (mm)	β ₂ °	β ₁ °	P(c.v)
	3495	118	24,5	5,5	5,5	17,6	46,5	1



Figure 1. Three-dimensional impeller design.

3.2 Mesh generation

After defining the fluid domain, it is possible to generate the mesh that is utilized in the simulation. For this, software is employed, which is found in the ANSYS WORKBENCH platform specialized in the mesh generation. The program allows the use of the methods and tools capable of the mesh refinement at the most critical points of the geometry that generates an appropriate level of refinement to the problem.

Figure 2 shows the three-dimensional mesh generation for the fluid domain and it contains 2962790 nodes and 2837225 tetrahedral elements.

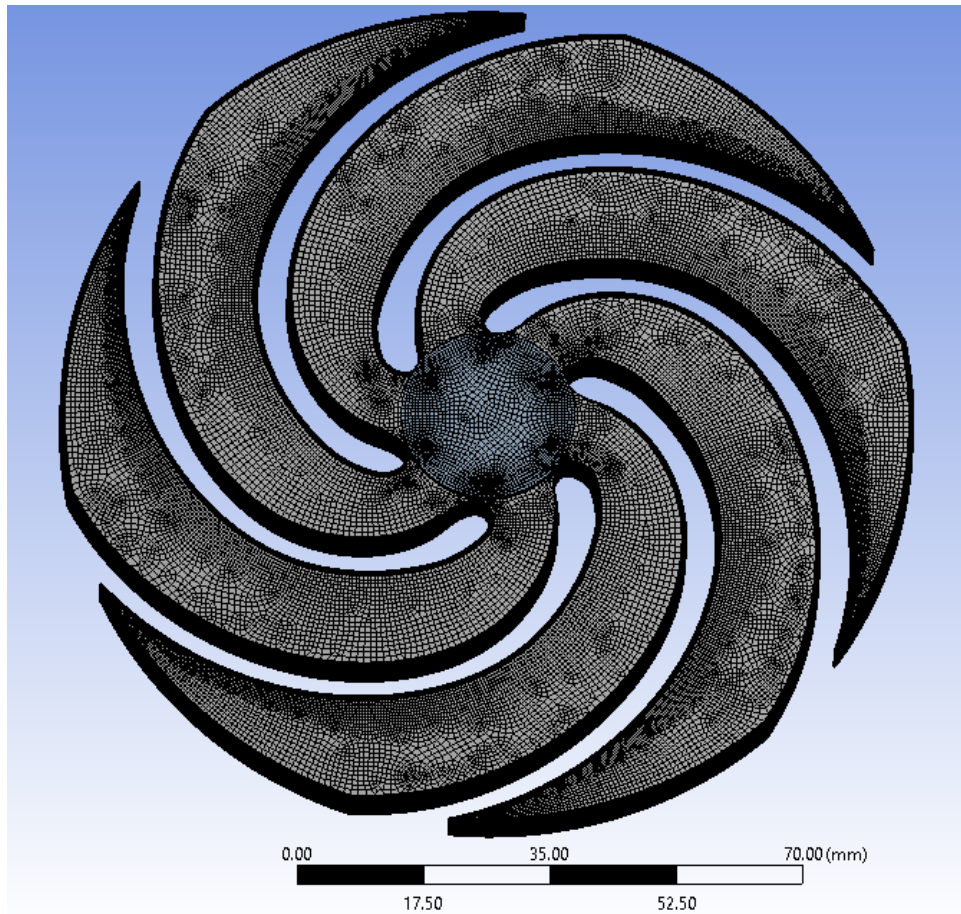


Figure 2. Impeller with fine mesh.

3.3 Boundary conditions

After the definition of the geometry and mesh, the parameters for the flow pattern and the fluid properties were determined. Initially, the z axis was selected as the reference for the rotational movement of the impeller or the fluid and a rotation speed of 3495 rpm was defined in the opposite direction of the blades. Simulations were performed using water ($\rho=1000 \text{ kg/m}^3$ e $\mu=8.899 \text{ mPa}\cdot\text{s}$) as the fluid of the current work. The flow was considered in steady-state and the reference pressure was adjusted to an atmosphere. The turbulence model chosen was the κ - ϵ , whose convergence criteria stipulated in minimum RMS residue of 1×10^{-6} .

In the simulated model, following boundary conditions were applied:

- Impeller input: The impeller input has been configured as “inlet” which is interpreted as the entrance that allows the fluid to enter into the system. The output of the input subdomain is an interface region with another rotating subdomain. It is applied for this boundary condition a mass flow rate which was changed in the simulation for each simulated point. Therefore, the change of this boundary condition that gives the desired analysis data for the results.

- Impeller output: The boundary where the fluid leaves the rotor has been configured as the “outlet”. This condition allows the fluid flows to the system output only. It is specified the reference of the zero atmospheric pressure. For all simulated points, this constant contour condition is considered.

- Walls: The walls are defined as the subdomain limited by the channels formed among the impeller blades. The boundary condition is applied to this boundary as “no slip” and impermeability, for this condition the velocity of fluid in the wall has the same velocity of the wall. In the simulations the walls have angular velocity. The flow pattern was set to be isothermal and the same temperature as the walls, thus could neglect the thermal exchange.

4. RESULTS AND DISCUSSIONS

Twelve simulations were performed for the fluid flow varying the mass flow rates for the construction of head characteristic curve for the impeller. The numerical results obtained by the simulations were compared with the results obtained analytically.

The analytical data for the total head were calculated by the Eq. (4), which according to Macintyre (1997) that corresponds to the Euler's pump equation.

$$H_e = \frac{u_2 v_{u2}}{g} \quad (4)$$

where u_2 is the circumferential velocity of the impeller output, v_{u2} is the circumferential component of the absolute velocity at the output and g is the gravitational constant.

Considering that the head of the impeller corresponds to the delivery head H_u , which is the energy given out for off-pump flow, and considering the losses from the hydraulic nature, it can be obtained by the pumping head in Eq. (5).

$$H_u = H_e \cdot \varepsilon \quad (5)$$

where ε is the hydraulic performance.

In the simulations performed, the most difficult part was observed for the points with low flow rate. This difficulty existed due to the formation of fluid recirculation zones in the region among the blades. Figure 4 and Tab. 3 show how the numerical and analytical head vary for the twelve flow rates applied.

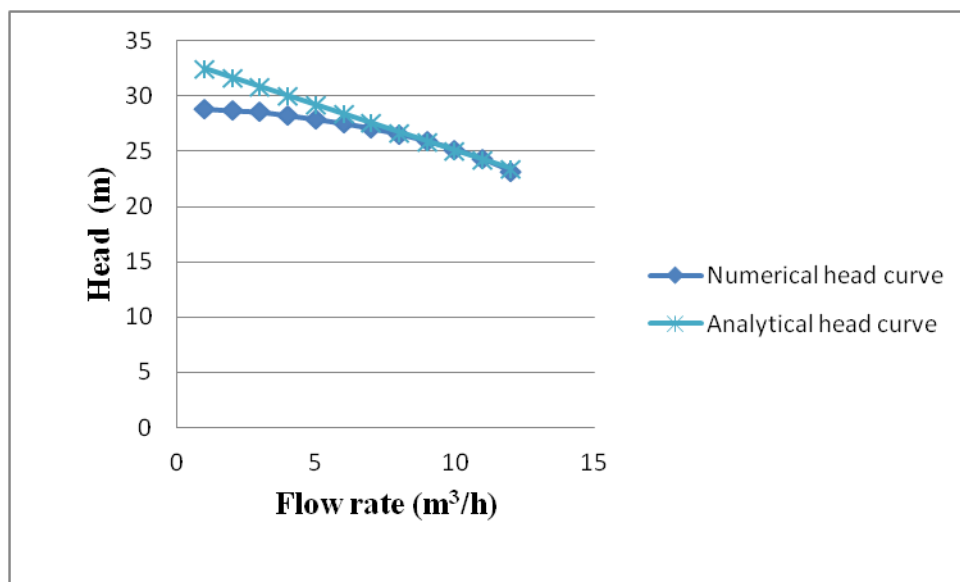


Figure 4. Head as function of flow rate.

Table 3. Analytical and numerical head data.

Simulation	Mass flow rate	Analytical head	Numerical head
	kg/s	m	m
1	0.27	32.48	28.87
2	0.55	31.65	28.71
3	0.83	30.83	28.58
4	1.10	30.01	28.26
5	1.38	29.18	27.93
6	1.66	28.36	27.55
7	1.93	27.54	27.10
8	2.21	26.71	26.57
9	2.49	25.89	25.95
10	2.76	25.07	25.21
11	3.04	24.24	24.31
12	3.32	23.42	23.24

Analyzing the results presented in Fig. 4 and Tab. 3, it can be observed that the trend of the numerical results are similar to the results obtained analytically, showing that the numerical model applied in the simulations provide satisfactory data in comparison to the theory applied.

4.1 Fluid flow analysis

For the certification of the results obtained and analyzed in this work comply with the turbulence model used in the simulations, the data of y^+ were evaluated. It can be observed in Fig. 8, the data is within the proper range proves the mesh produced and used in the simulations is appropriate to the model.

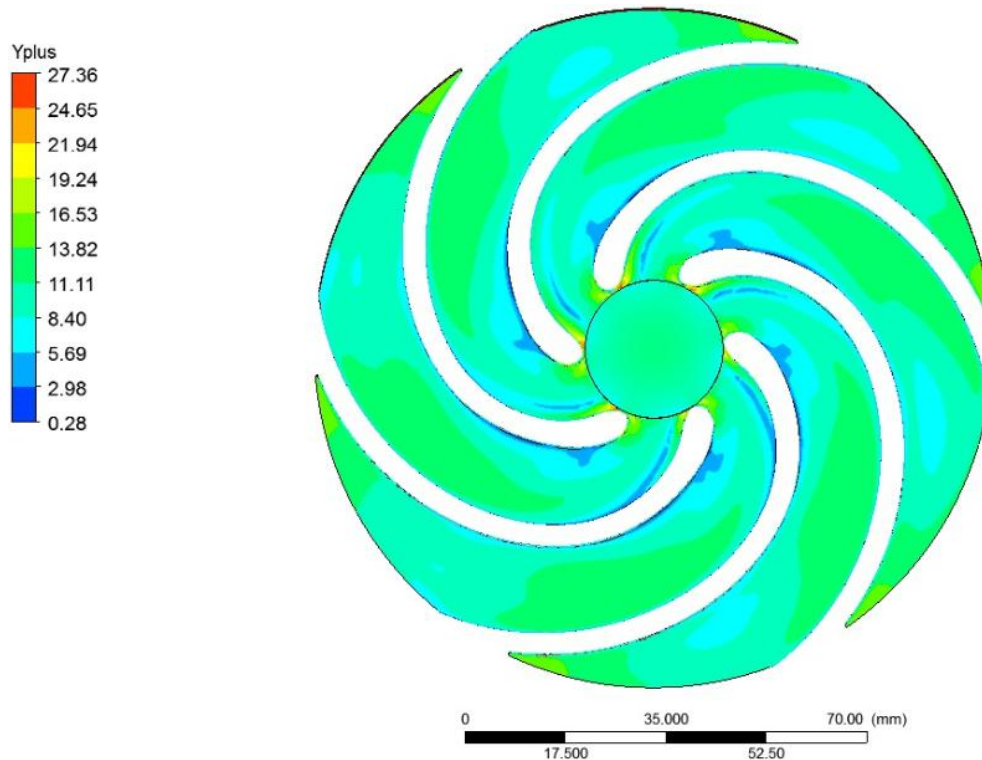


Figure 8. Variation of y^+ for a flow rate of $10 \text{ m}^3/\text{h}$.

In the evaluation of the pressure and velocity distribution, it was chosen the results obtained from the simulation performed for a mass flow rate of $10 \text{ m}^3/\text{h}$ which is near to the pump operating point and it is according to the characteristic curves of the pump supplied by the manufacturer with the flow rate of $10.6 \text{ m}^3/\text{h}$.

Figure 5 shows the pressure variation for the fluid flow within the impeller. The pressure distribution in the blade channel demonstrates a gradual pressure increase, from the center to the periphery, proving the energy transfer inside and attending the final conditions to the process. The pressure increase is caused by a decrease in velocity through a progressive increase in the fluid flow area in the direction from the inlet to the outlet of the channel.

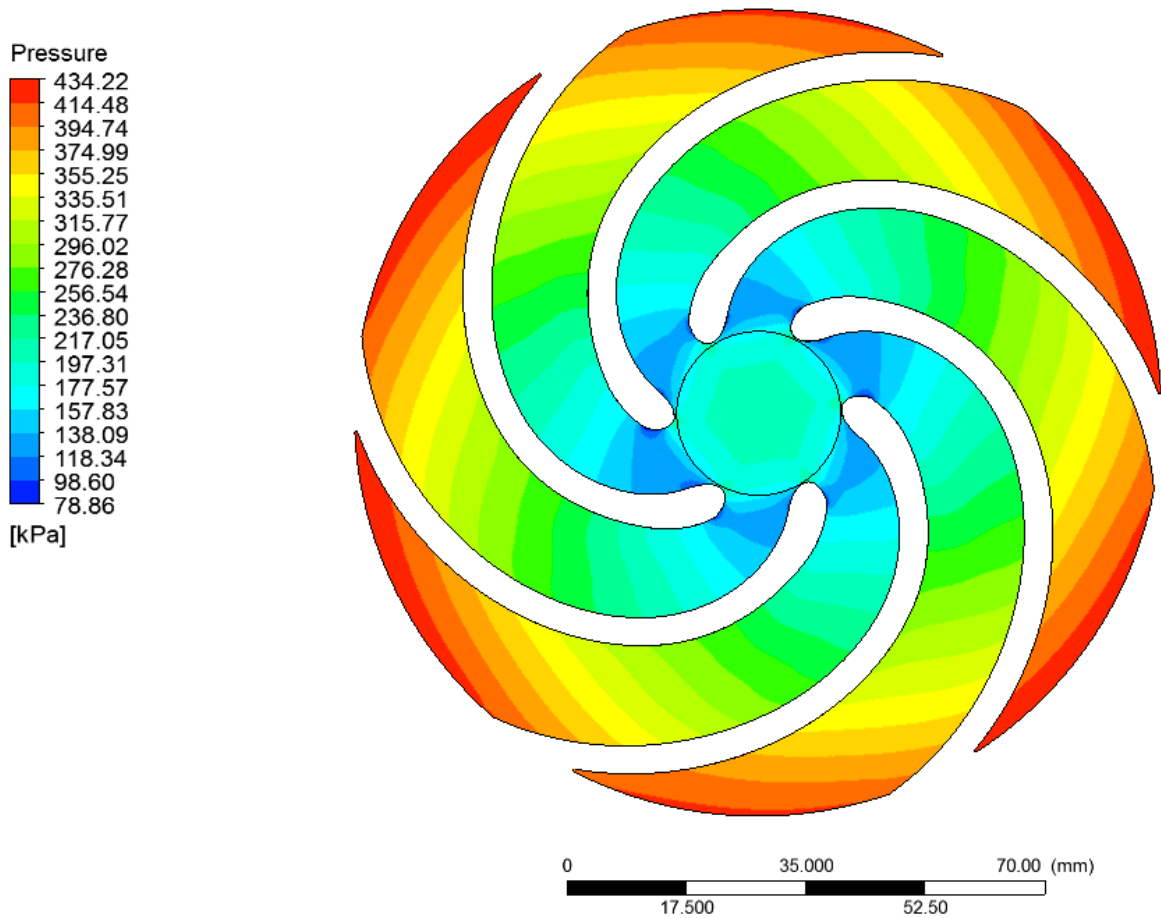


Figure 5. Pressure distribution of impeller for a flow rate of $10 \text{ m}^3/\text{h}$.

Figure 5 shows the pressure reducing by the inlet of the channel, it is probably caused by a sharp curvature in the geometry causing energy losses. By evaluating two points of the same circumference which starts from the output of the impeller entrance, there is a higher pressure on the face of the blades and consequently, a lower pressure on the lower camber in the blades. It happens because of the inertia that the liquid to be diverted from its trajectory. In addition, the number of blades is relatively small, so the trajectory of the liquid fillets is not strictly parallel to the profile of the blades, as is shown by Fig. 6.

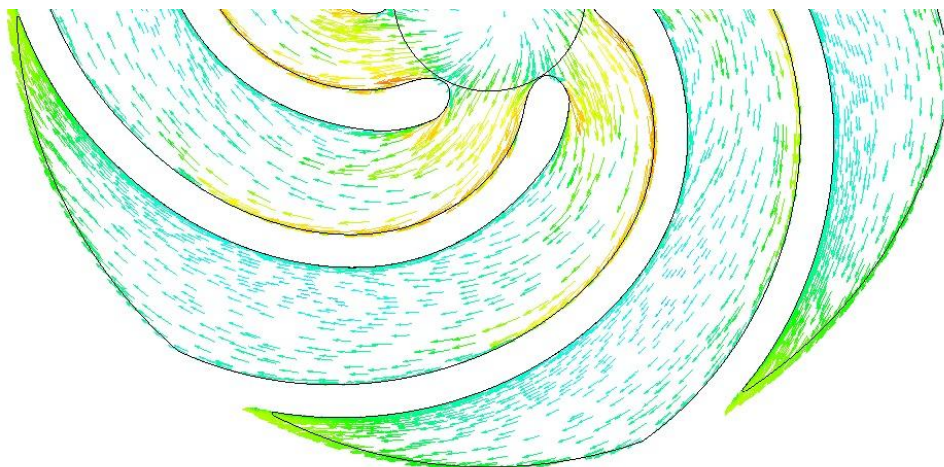


Figure 6. Velocity vector distribution of impeller for flow rate of $10 \text{ m}^3/\text{h}$.

The velocity variation in the flow inside of the impeller is shown in Fig. 7. The velocity decreases as the flow area increases producing a gradual addition of the pressure required for the pump to fulfill its function.

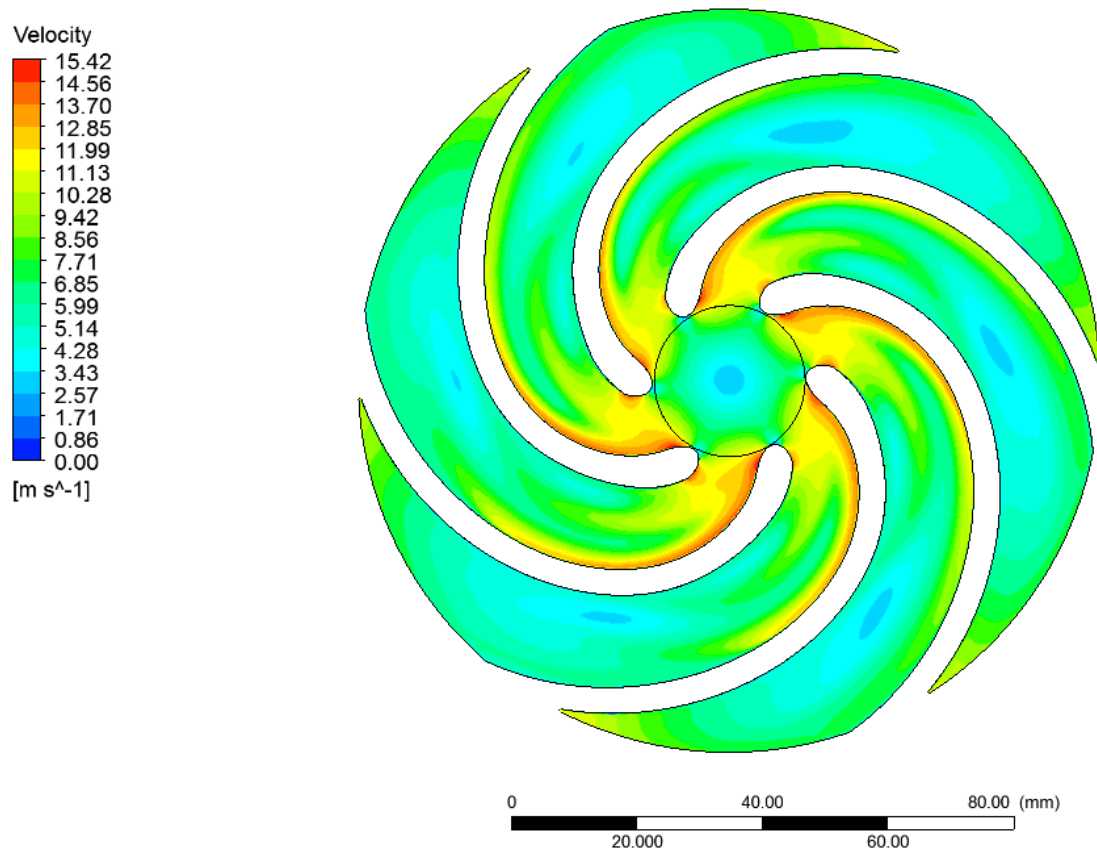


Figure 7. Velocity distribution of impeller for a flow rate of $10 \text{ m}^3/\text{h}$.

As is shown by Fig. 7, at the entrance region of the blade there is an increase of the velocity that extends in lower camber. This is due by the rotation movement that the liquids receive through the impeller that the liquid subject to the centrifugal force that promotes the displacement of the particles towards to the periphery of the impeller. Pressure distribution is compared with velocity distribution in the fluid flow and it can be stated that in the regions where the higher pressure field regions are observed where the lowest velocities are found.

5. CONCLUSIONS

In the work developed were carried out simulations considering the geometry of centrifugal pump impeller that is based on a pump available in Turbomachinery Laboratory from URI/RS. The results obtained are preliminary and have the purpose of assisting in the realization of new simulations on an impeller obtained from pumps design.

Simulations performed on the impeller geometry and the results inferred for the internal flow in the pump channel were used to obtain the head characteristic curves and to compare with the analytical results. In addition, the fluid flow analysis was carried out by studying the meridional profile corresponding to a flow rate close to the pump operating point in consequence to verify the pressure and velocity conditions inside the impeller.

The results from this study show that head characteristic curves are a good agreement when compared to the analytical results, it demonstrates that the use of CFD for flow characterization and analysis on the performance of the centrifugal pump impeller is itself a useful and reliable tool.

It can be also observed that the data of y^+ obtained in the simulation are within the appropriate range which shows that the results achieved comply with the requirements of the turbulence model and the mesh applied is adequate to the problem.

By evaluating the internal flow on the impeller through the pressure and the velocity profiles, it can be concluded that the energy transfers inside of it due to the gradual pressure increases of the channel between the blades which comply with the requirements necessary for the pump to perform its function. Furthermore, it can be seen a zone of higher pressure on the leading edge and consequently compared to lower camber of the blades due to the resistance of the fluid leaving its path, the speed not being strictly parallel to the profile of the blades.

6. ACKNOWLEDGEMENTS

This work was supported by CAPES, the Laboratório de Dinâmica de Fluidos Computacional (CFD) at Universidade Federal Rio Grande do Norte, and the Laboratório de Máquinas de Fluxo da Universidade Regional Integrada do Alto Uruguai e das Missões (URI) in Rio Grande do Sul for sending the impeller geometry applied for this paper.

7. REFERENCES

- Macintyre, A. J., 1997. *Bombas e instalações de bombeamento*. LTC, Rio de Janeiro, 2ª edição.
- Maitelli, C. W. S. P., 2010. *Simulação do Escoamento Monofásico em um Estágio de uma Bomba Centrífuga Utilizando Técnicas de Fluidodinâmica Computacional*. Tese de Doutorado, Universidade Federal do Rio Grande do Norte, Natal.
- Mattos, E. E., Falco, R., 1998. *Bombas industriais*. Interciência Ltda, Rio de Janeiro, 2ª edição.
- Segala, W., 2010. *Simulação Numérica do Escoamento Monofásico no Primeiro Estágio de uma Bomba Centrífuga de Duplo Estágio*. Dissertação de Mestrado, Universidade Tecnológica Federal do Paraná, Curitiba.
- Wenzel, G. M., 2010. *Análise numérica da esteira de turbinas eólicas de eixo horizontal: estudo comparativo com modelos analíticos*. Dissertação de Mestrado, Escola de Engenharia da Universidade Federal do Rio Grande do Sul, Porto Alegre.

8. RESPONSIBILITY NOTICE

The authors are the only responsible for the printed material included in this paper.